Removal of Hazardous Material from Wastewater by using Metal Organic Framework (MOFs) Embedded Polymeric Membranes

Gnanaselvan Gnanasekaran[a], Sasikumar Balaguru[a], Arthanareeswaran Gangasalam[a]*, Diganta B Das[b]

[a]Membrane Research Laboratory, Department of Chemical Engineering, National Institute of Technology, Tiruchirappalli, Tamil Nadu, India. PIN-620015.

[b]Department of Chemical Engineering, Loughborough University, Loughborough, UK

Email.id: arthanaree10@yahoo.com

ABSTRACT

Heavy metals in wastewater can cause acute and chronic toxicity which leads to learning disabilities, cancer, and even death. In present work, Zn based MOF (MOF-5) was prepared, and it is characterized by FT-IR, XRD, and SEM Analysis. MOF-5 incorporated polymeric membranes (PES, CA and PVDF) prepared by phase inversion method. The morphology, hydrophilicity, porosity, permeation performance, antifouling properties and the rejection of Cu (II) and Co (II) metal ions of the membranes were significantly improved with the addition MOF-5. Higher rejection efficiency for Co (II) in PES/MOF-5 and CA/MOF-5 was found to be 74.40 % and 77 % respectively.

Keywords: Heavy metal ions, Metal-organic frameworks (MOFs), Composite membranes, Nanofiltration (NF).

Introduction

Increasing contamination of indsutrial wastewater by heavy metal ions found to be significant global concern. The primary source of heavy metal ions are industries like electroplating, battery manufacturing, metallurgical, tannery, and metal finishing. [1,2] Unlike organic contaminants, heavy metal ions are non-biodegradable in nature and likely to cause healthy risk by entering into the human food chain through marine animals. [3, 4] Over the years, numerous techniques have been studied for the removal of heavy metal from wastewater namely adsorption, precipitation, ion exchange, membrane separation, electro dialysis, and photocatalysis. [5] Nanofiltration (NF) membrane was proven to be a very potential method for removal of heavy metals because of its low cost and high effectiveness. [6] A comparative study of copper and cadmium removal from wastewater using NF has been investigated. [7] NF membranes were shown to be capable of removing 96% of copper and 97% of cadmium ions. However, the difficulties to achieve both high water permeability and rejection simultaneously limits the performance of NF membranes.

Metal-organic frameworks (MOFs) are proven to be a promising material to overcome the above mentioned drawback. MOFs offers highly tunable pore structure, along with an enormous variability and chemical functionality. [8] MOFs can be synthesised by combination of metallic and organic linkers namely benzenedicarboxylates (BDC) and benzetricarboxylates (BTC) via chemical or physical techniques. The incorporation of MOFs on polymer matrix has been reported for the removal of dye and heavy metals using nanofiltration. [9,10] Thin film nanocomposite membranes were developed by embedding MOFs on Polyimide support shows increased permeability of solvent due to increase in porosity and hydrophilicity. [9] UiO-66@GO/PES composite membranes has been reported with enhanced antifouling property. The pure water flux of MOFs incorporated composite membrane was increased by 351%

compared to that of neat PES membrane, together with increased rejection ratio to organic dyes. [11] The MOFs were used for the removal of heavy metal ions from aqueous solution. Bakhtiari [2] and Rivera *et al*., [12] proven that MOF-5 can be an effective adsorbent for the removal of heavy metal ions like copper and lead from aqueous medium. Therefore, research on MOF embedded polymeric membrane is highly desirable, especially for the application of water purification. [10] Despite these considerable advantages, limited structural stability of MOFs when exposure to water remains a point of concern. The water stability of MOFs related to composition of metal sites and structure of metal clusters. [13] Polymer and MOFs is controlled by weak interactions such as Hydrogen bond, van der Waals forces, and π-π stacking. MOFs introduces free volume and active porous sites on the membrane will be favourable for gas and liquid separation. [14] Herein, we report MOF-5 embedded membranes with three different polymers namely Cellulose acetate (CA), Polyethersulfone (PES), and Polyvinylidene fluoride (PVDF). MOF-5, a prototypical Zn based MOF with cubical structure have been used to achieve the high water purification performance for the removal of copper and cobalt ions (hazardous materials**)** from wastewater. The schematic representation of removal of heavy metal ion from aqueous solution by MOF-5 incorporated polymeric membranes Nanofiltration is shown in Scheme. 1.

Experimental

Materials

N, N-dimethylformamide (DMF, Merck), Terephthalic acid (SRL Pvt Ltd., India), Zinc nitrate hexahydrate (Loba Chemie Pvt Ltd. India) were employed to prepare the MOF material. All chemicals used were of analytical grade. Copper sulphate pentahydrate ($CuSO_4 .5H_2O$), Cobalt sulfate hexahydrate ($CoSO_4 .7H_2O$) were purchased from Merck specialties Pvt Ltd., India. Polyethersulfone (PES, veradel 13000 p), Polyvinylidene fluoride (PVDF, Solef® 6010) was procured from Solvay Solexis Ltd., India. Cellulose Acetate (CA) were purchased from Mysore

Acetate and Chemicals Company Ltd., India. Ultrapure water was produced in the laboratory using millipore pilot plant.

Preparation and characterization of MOF-5

MOF-5 was synthesized in a glass reactor equipped with reflux condenser following the procedure reported in the literature. [9,15] 2 g of terephthalic acid and 9.31 g of zinc nitrate hexahydrate were dissolved in 60 ml of DMF solution under stirring at atmospheric conditions and heated up to 150°C for 4h. After 2 hr, white crystals of MOF-5 was formed, and the product was cooled down to room temperature. The white crystals were separated by filtration and washed with 100 ml acetone, and finally, solid crystals were dried at 60°C for 3 hr in a vacuum oven. Fourier transform infrared (FTIR) spectroscopy of MOF-5 (Thermo Scientific Nicolet iS5 FT-IR spectrometer) was analysed in the spectral region of wavenumbers from 400 to 4000 cm^{-1}. The crystalline structure of MOF-5 was studied using X-ray diffractometer (Model Rigaku Ultima III) using a monochromatic source of Cu Kα radiation with the range of 2Θ with an angle of 5° to 80° and with an operating voltage of 40 kV. The surface morphology of prepared MOF-5 was studied using Scanning Electron Microscope equipped with Energy Dispersive X-ray (Quanta 250 FEG).

Fabrication of MOF incorporated polymeric membranes

The neat and MOF-5 embedded PES, CA, PVDF membranes were prepared by phase inversion induced by immersion precipitation method. [8] MOF-5 loading was kept at 0.5% of the polymers. The casting solutions contain 17.5% of polymers (PES, CA, and PVDF) and 21.7 ml of DMF solvent. The composition of casting solutions for all the membranes is shown in Table 1. MOF-5 (0.5%) was added into 21.7ml of DMF and dispersed well by sonication for 1 hr to improve the homogeneity using Ultrasonicator. After dispersing MOF-5 in DMF, polymers were dissolved in the dope solution by mechanical stirring for about 3 hr. The

complete dispersion of Polymer/MOF-5 was again confirmed using ultrasonication for 30 min before casting. After removing air bubbles, homogenous casting solution was cast onto a finely levelled glass plate with 400 μm thickness. Subsequently, the film was then immersed in the distilled water which is maintained at 10°C, and then membranes were soaked in fresh distilled water for 24 hr to ensure the complete phase inversion.

Membrane Characterisation

The functional group of neat and MOF-5 incorporated polymeric membranes (PES, CA and PVDF) were investigated by ATR interfaced Fourier transform infrared (FTIR) spectrophotometer (Thermo Scientific Nicolet iS5 FT-IR spectrometer, India). The range of wavenumbers were analysed between 400 to 4000 cm^{-1}. The XRD pattern of membranes were analysed by X-ray diffractometer (Model Rigaku Ultima III) using a monochromatic source of Cu Kα radiation with the range of 2Θ with an angle of 5° to 80° and with an operating voltage of 40kV.The surface morphology of neat polymer and composite Polymer/MOF-5 membranes were studied using Scanning Electron Microscope equipped with Energy Dispersive X-ray (VEGA 3, TESCAN, USA). The membrane samples were fractured in liquid nitrogen, and gold coated by sputtering to make them conductive. The MOF-5 distribution on the surface of the composite membrane has been analysed by Energy Dispersion of X-ray (EDX).

Hydrophilicity of membranes were measured using contact angle measurement. Goniometer (model 250-F1 Rame-Hart Instruments, Succasunna, NJ) used for the determination of Contact angle for membranes by sessile drop method using. About 5 μL drop of water is injected on a dry membrane surface at five different locations through a micro syringe. The average of contact angle value was measured from the individual droplets in the five regions which determine the hydrophilicity of membrane.

Permeation and rejection studies

The permeability of neat and MOF-5 incorporated polymeric membranes were studied by using pure distilled water and aqueous solutions of Cu (II), Co (II) at a concentration of 1000 ppm. The permeation studies were conducted by using a dead end stirred NF cell with an active membrane area of 14.6 cm^2.The water was pressurized by supplying nitrogen gas to the NF cell, and then membranes were compacted for 30 min at 10 bar pressure to minimize the compaction effects. At steady state conditions, the water permeated for 10 min at 25°C were noted down, and the permeate flux (J_w) of each membrane was quantified based on the following Eq. (1).

$$J_w = \frac{\mathrm{V}}{\mathrm{A} \times \Delta \mathrm{t}} \qquad (1)$$

where J_w is the permeate flux (kg/m^2hr), V is permeate volume (m^3), A is effective membrane area (m^2), and Δt is permeation time (hr).

The performance of neat and composite membranes was evaluated using percentage rejection of heavy metal ions from aqueous medium. The concentration of permeate solutions was determined by using Atomic absorption spectrophotometer (Perkin Elmer, Analyst 4000, USA). The measured value of permeate (C_p) and feed concentration (C_f) was used to calculate observed rejection percentage (R_{obs} %) by following the Eq. (2).

$$\mathrm{R_{obs}}(\%) = \left(1 - \frac{\mathrm{C_p}}{\mathrm{C_f}}\right) \times 100 \qquad (2)$$

Membrane Resistance (R_m)

The resistance to the feed flow of neat and MOF-5 incorporated polymeric membrane has been calculated by Eq. (3).

$$\mathrm{R_m} = \left(\frac{\Delta \mathrm{P}}{\eta_\mathrm{w} \times \mathrm{J_w}}\right) \qquad (3)$$

Where,

154 ΔP - Transmembrane Pressure.

155 η_w - Viscosity of the feed.

156 ***Membrane porosity and pore size***

157 To measure the membranes porosity, samples were cut into specific sizes and then mopped
158 with filter paper. After noting their wet weight, the samples are dried in an oven at 60°C for 24
159 hr. The porosity (ε) and mean pore radius of the membranes were calculated by [Eqn. 1], and
160 [Eqn. 2] respectively in the Supporting Information.

161 ***Determination of Mass Transfer Coefficient and Diffusion Coefficient***

162 Due to concentration polarisation, the solute concentration at membrane surface (C_m) is higher
163 than that of the bulk solution concentration (C_f). This leads to additional resistance to the
164 permeate flux (J_v), and it can be expressed based on the Concentration Polarisation Model
165 described in the Supporting Information [Eqn. 3]. Correlation for the mass-transfer coefficient
166 can be obtained based on the diffusive transport of the heavy metal ions described in the
167 Supporting Information [Eqn. 4]. The diffusivity of an aqueous solution of Cu (II) and Co (II)
168 was found to be 4.335×10^{-9} m^2/s, 4.182×10^{-9} m^2/s respectively, and listed in Table 2. Observed
169 rejection efficiency of heavy metal ions were affected by the concentration polarisation, and
170 hence, the real rejection percentage of the membranes can be calculated using the concentration
171 at the surface of the membrane (C_m) by [Eqn. 6], in the Supporting Information.

172 **Results and Discussion**

173 ***FTIR characterization of MOF-5***

174 The FTIR spectra of MOF-5 shown in Fig. 1. Asymmetric stretching of C-O bonded to Zn has
175 been identified by the attachment of carboxylate ligand to Zn_4O centre were indicated in the
176 peaks of 1381 And 1573 cm^{-1}. The peak values between the range of 900 to 1250 cm^{-1} has
177 various small peaks are appeared to indicate the C-H stretching of benzene dicarboxylate

178 linker. The broad peak occurred in the range of 3161 cm^{-1} shows the O-H group IR bands at
179 1502, and 653 cm^{-1} indicated random dimethylformamide (DMF) distribution in the MOF-5
180 framework structure. [17]

181 ***XRD analysis of MOF-5***

182 X-ray diffraction analysis of MOF-5 shown in Fig. 2. The peaks at 6.8°, 9.7°, 14° and 15.8° in
183 2θ which indicates the formation of a crystalline structure. [17] The inconsistency peaks appear
184 due to the framework interpenetration and pore occupation. The intensities of the two peaks
185 were overturned that can be attributed to some alterations of atomic orientations in the crystal
186 planes by absorbed species (solvent and water molecules), unreacted zinc centers and
187 framework interpenetration.

188 ***Surface Morphology of MOF-5***

189 Surface morphology of MOF-5 have shown using SEM images in Fig. 3. Irregularly shaped,
190 the majority had the cubic shape with crystals structure and porous nature, its present in the
191 (Fig. 3a and 3d). [17] The cubical structure has occurred more, and some cluster-like
192 arrangement also present which shows the adsorption property of MOF-5, its shows in the (Fig.
193 3b and 3c). The organic cluster and inorganic moiety interaction have occurred in MOF-5.

194 ***Energy Dispersive X-ray Spectroscopy of MOF-5***

195 The elemental composition of the MOF-5 was characterized by EDX (Fig. S1, Supporting
196 Information) revealing the expected elemental constituents (C, Zn, and O) are detected. The
197 peak appearance indicate the Zn metal ion attach with carboxylate ligand and it proves the
198 formation of MOF-5 by the interaction of metal ion and organic cluster. [17]

199 ***FTIR characterisation of membranes***

The FTIR spectra of neat and MOF-5 incorporated polymeric membranes namely PES/MOF-5, CA/MOF-5, and PVDF/MOF-5 were illustrated in Fig. 4. The spectral features of neat PES, CA and PVDF membranes are repeated in composite CA/MOF-5, PES/MOF-5 and PVDF/MOF-5 membrane spectra, in which peaks corresponding to MOF-5 were also observed. The peak values for both neat PES and PES/MOF-5 at 1240, 1485, and 1578 cm^{-1} have identified the bands of aromatic ether, C=C bond stretch and aromatic bands of the benzene ring respectively which confirms the characteristic peaks of PES. The presence of the peak value at 3370 cm^{-1} in PES/MOF-5 membranes indicates the (O-H) stretching of MOF-5 in the PES membranes. [18] In case of neat CA and CA/MOF-5 membranes the peak at 1746 cm^{-1} was identified the stretching of carbonyl group has been present in both membranes and for composite CA/MOF-5 membrane the peak occurred in the range of 3460 cm^{-1} shows the O-H stretching which indicates the presence of MOF-5 in the membranes. [19] Band at wavenumbers 1396 cm^{-1} and 1175 cm^{-1} is due to CH stretching vibration and C-F stretching vibration in PVDF and PVDF/MOF-5 membranes. The broad peaks occurred at 3429 cm^{-1} in FTIR spectra of PVDF/MOF-5 could be assigned to O-H stretching. [20] From these functional group identification, confirms MOF-5 is embedded into membranes and create a polymeric structure as an integral part, could be enhancing the hydrophilic nature compared with neat membranes.

XRD analysis of membranes

The XRD diffraction patterns of MOF-5, neat and MOF-5 incorporated polymeric membranes were shown in Fig. 5. The XRD spectra of MOF-5 had two peaks at 9.8° 2θ and 15.8° 2θ, which confirm the crystallinity of MOF-5 particles. The peak occurrence of little shift at 9.8° 2θ in the composite PES/MOF-5, CA/MOF-5 and PVDF/MOF-5 membranes in the dispersion peak of PES, CA and PVDF membranes due to the low addition of MOF-5. It's indicated that the slight interaction between MOF-5 and polymeric membranes. [21] It is confirmed that the

synthesized MOF-5 improve the stability, hydrophilicity and antifouling properties of composite polymeric/MOF-5 membranes. [21,22] XRD analysis indicate that the MOF-5 presence in the Polymeric membrane matrix

Surface morphology of membranes

The surface morphology of the neat and MOF-5 embedded CA, PES, PVDF membranes was monitored by SEM images. The cross-sectional view of neat and modified PES membrane is shown in Fig. 6. It is well known that the skin layer and porous sublayer in the membrane determine the water permeation rate and separation factor. [23] The thick and dense asymmetric structures were observed on neat PES membrane such morphology was responsible for the lower pore radius and membrane permeability. In case of modified PES membrane, the interconnection between skin top layer and substructure (bottom layer) were improved. Finger-like substructures and thin skin layer were observed. Subsequently, increase in pore radius and decreased macro voids were found with the addition of 0.5 wt. % of MOF-5.

The asymmetry structure of sponge-like cross-section, finger-like and highly porous structure was observed in the surface morphology of neat CA and CA/MOF-5 in Fig. 7. The MOF-5 has been uniformly dispersed in the polymeric membranes, and the structure of the MOF-5 incorporated membranes does not differ from the neat membranes due to the low-level loading 0.5 wt. % of MOF-5 into the membranes. Defective pore structure has been occurred due to the interfacial stresses of MOF-5 and membranes. [22] The increase in the pore size indicated the increased hydrophilicity and permeability for CA/MOF-5 which improves the membrane to be a perfect membrane for the removal of heavy metal ions. Fig. 8 shows the cross sectional view of neat PVDF and PVDF/MOF-5 membranes. An asymmetric structure consisting of a dense top layer, a porous sublayer (support), and a sponge-like structure in the bottom layer. It seems that the support layer begins with finger-like cavities underneath the dense top layer ending up in large voids near the bottom layer. In the pristine membrane, a significant portion

of sublayer is made of a spongy structure consisting of small cellular pores, and only little finger-like voids were observed underneath the top surface. While the addition of 0.5 wt. % of MOF-5 into the PVDF casting solution the finger-like voids have been developed nearly up to the membrane bottom, and the share of spongy pores is lower by increasing the hydrophilicity of PVDF membranes. Porosity was enhanced by the addition of MOF-5 in the casting solutions of PVDF membrane. [24] This trend can be interpreted and explained by membrane formation mechanism during phase inversion process into the coagulation bath. MOF-5 in the casting solution increases the penetration of nonsolvent (water) into the casting solution.

Energy Dispersive X-ray Spectroscopy of membranes

The presence of organic elements in both neat and MOF-5 incorporated Polymeric membranes, indicates that the presence of MOF-5 does not affect the asymmetric membrane structures. The MOF-5 embedded polymeric membranes shows only minor percentage of Zn elements could be due to the low percentage loading of MOF-5 (Fig. S2, Fig. S3, and Fig. S4, Supporting Information). The presence of Zn element in the MOF-5 incorporated polymeric membranes confirms the presence of MOF-5 in the polymeric matrix. [25]

The Porosity and Average Pore Radius of Membranes

The porosity and mean pore radius values were shown in Table. 3. The average pore radius of PES/MOF-5 membrane has been increased from 5.62 nm to 6.97 nm, and the porosity (%) value also increase from 70 % to 78 % due to the addition of MOF-5 into the PES casting solution and its obviously shows that MOF-5 has improved the hydrophilicity of PES. [26] The average pore radius of CA/ MOF-5 membrane has been increased from the range of 5.57 nm to 9.09 nm due to the addition of MOF-5 which improve the hydrophilicity of CA membranes and porosity (%) also increased from 72 to 81 %. [22] The average pore radius of PVDF/MOF-5 has been raised from the range of 3.92 nm to 4.3 nm with the addition of MOF-5. [26]

Hydrophilicity Measurement

The hydrophilicity of the membranes characterized by the contact angle measurement and the contact angle data are listed in the Table. 4. The contact angle falls with the addition of MOF-5, and this could be due to fact that contact angle is a function of surface roughness. The contact angle of PES membranes decreased from 86.075° to 76.42°, with the addition of MOF-5 which shows that the hydrophilicity PES/MOF-5 membranes significantly superior to neat PES membranes. [27] In case of CA, PVDF membranes contact angle was decreased from 75.03° to 70.68° and 80.47° to 72.975 ° respectively, which proves that hydrophilicity has been increased because of the addition of MOF-5. [19,24]

Membrane Resistance and Permeability

The pure water flux of neat and MOF-5 embedded PES, CA and PVDF membranes can be used to determine the hydraulic permeability and membrane resistance. The pure water flux of neat and MOF-5 incorporated polymeric membranes is shown in Fig. 9. The membrane permeability is inversely proportional to the membrane resistance. The membrane permeability and membrane resistance was calculated from Eq. (1), and Eq. (3) respectively and listed in Table.5. The neat PES, CA and PVDF membranes were having higher membrane resistance compared with PES/MOF-5, CA/MOF-5 and PVDF/MOF-5 could be due to the increase in hydrophilicity of membranes by addition of MOF-5. [27] For PES membrane, the permeability has been increased from 29.52 ±1.6 L/m^2 hr to 53.31± 1.6 L/m^2 hr and consequently membrane resistance was decreased from 13 ×10^{13} m^{-1} to 7.4×10^{13} m^{-1}. In case of CA/MOF-5 permeability was increased from 41.01±1.2 L/m^2 hr to 69.72± 1.4 L/m^2 hr and the hydraulic resistance was reduced from 9.6×10^{13} m^{-1} to 5.6×10^{13} m^{-1} which indicates that the hydrophilicity of CA/MOF-5 membrane has been improved. [19,22] The PVDF/MOF-5 have higher water flux compared to neat PVDF membrane, and hydraulic resistance value was

298 reduced from 17×10^{13} m^{-1} to 11×10^{13} m^{-1}. [24] CA/MOF-5 has shown higher water flux
299 compared to all other membranes, possibly due to the higher porosity of the CA membranes as
300 observed in Table 3. In all cases, MOF-5 incorporated membranes exhibited higher fluxes than
301 their corresponding neat membranes. The addition of MOF-5 particles to membranes enhances
302 the pure water flux through them, due to the increased hydrophilic character of the membranes.
303 Increase in hydrophilicity could be due to the higher affinity of metal cluster of MOFs for water
304 and consequently the pure water flux also increased.

305 ***Heavy Metal Ions Permeability of Membranes***

306 Experiments were carried out for the removal of copper Cu (II) and cobalt Co (II) metal ions
307 from water to study the influence of MOF-5. Fig. 10 and Fig. 11 illustrates the variation of the
308 rejection of neat and composite MOF-5 membranes for the metal ion aqueous solutions
309 containing Cu (II) and Co (II) respectively. CA/MOF-5, PES/MOF-5, and PVDF/MOF-5
310 membranes has higher permeability flux of 59±1.2 L/m^2 hr, 41±1.6 L/m^2 hr and 27±1.4 L/m^2
311 hr respectively for Cu(II) solution when compared to neat CA, PES, and PVDF membranes. In
312 case of Co (II) solutions, similar higher permeability flux of 47±1.2 L/m^2 hr, 40±1.4 L/m^2 hr
313 and 24±1.2 L/m^2 hr observed for MOF-5 blend polymeric membranes CA/MOF-5, PES/MOF-
314 5, and PVDF/MOF-5 respectively, which proves that the MOF-5 enhance the hydrophilicity
315 and reducing the fouling flux. [28,29] CA/MOF-5 membranes has higher permeability compared
316 with all other membranes.

317 ***Performance of Composite Polymer/MOF-5 Membranes on heavy Metal ion rejection***

318 The effect of MOF-5 on the percentage rejection of metal ions for membranes is shown in
319 Table 6. The rejection capability of the prepared composite PES/MOF-5, CA/MOF-5
320 PVDF/MOF-5 membranes was comparatively higher than the neat membranes. The observed
321 rejection of Cu (II) in neat CA and CA/MOF-5 is found to be 50.8% and 53.3% respectively.

For PVDF and PVDF/MOF-5 observed rejection was 54.3% and 52.3%. The highest observed rejection of Cu (II) is obtained in CA/MOF-5 membranes which is due to the higher affinity of MOF-5 with the CA membrane. The Co (II) rejection is shown in Table.7. Rejection performance of prepared membranes for Co (II) is much higher than that of Cu (II).Higher rejection efficiency for Co (II) in PES/MOF-5 and CA/MOF-5 was found to be 74.40% and 77.0% respectively, which shows that membranes selectivity was not compromised with that of the flux. Hence both the rejection and the permeability flux of composite PES/MOF-5, CA/MOF-5, and PVDF/MOF-5 membranes remains higher than those of the neat polymeric membranes. [27] The real rejection efficiencies (R_{real}) of the heavy metal ions were calculated for both neat and Composite PES/MOF-5, CA/MOF-5, and PVDF/MOF-5 membranes. It was implied that R_{real} values of both neat and Composite PES/MOF-5, CA/MOF-5, and PVDF/MOF-5 membranes, remained higher than the R_{obs} values. [28] This is due to concentration polarisation, and it remains higher for dead-end NF cell.

Conclusion

The MOF-5 synthesized by simple Solvothermal method and characterised by FTIR, XRD analysis, SEM with EDX. Surface morphology reveals the formation of cubical structure of MOF-5 and its useful properties for the removal of heavy metal ions from wastewater. The MOF-5 particles incorporated into the three different polymers namely PES, CA and PVDF. The addition of MOF-5 in polymeric membranes influenced porosity and surface mean pore size of the prepared composite membranes. Further, the hydrophilic properties and performance of composite membranes enhanced by the incorporation of MOF-5 due to the metal clusters of MOF-5. The incorporation of MOF-5 has offered increased hydrophilicity of polymeric membranes and is confirmed by the 70%, 80.58% and 46.47% improvement in permeability for CA, PES and PVDF membranes respectively with 0.5 wt. % loading of MOF-5. The MOF-5 incorporated polymeric membranes (PES/MOF-5, CA/MOF-5, and

PVDF/MOF-5) has higher rejection efficiency of Cu (II) and Co (II) ions compared to neat polymeric membranes.

References

[1] Fu, F.; Wang, Q. (2011) Removal of heavy metal ions from wastewaters: a review. *Journal of environmental management*, 92 (3): 407-418.

[2] Bakhtiari, N.; Azizian, S. (2015) Adsorption of copper ion from aqueous solution by nanoporous MOF-5: a kinetic and equilibrium study. *Journal of Molecular Liquids,* 206: 114-118.

[3] Babel, S.; Kurniawan, T. A. (2004) Cr (VI) removal from synthetic wastewater using coconut shell charcoal and commercial activated carbon modified with oxidizing agents and/or chitosan. *Chemosphere,* 54: 951–967.

[4] Wan Ngah, W.S.; Hanafiah, M.A.K.M. (2008) Removal of heavy metal ions from wastewater by chemically modified plant wastes as adsorbents: A review. *Bioresource Technology,* 99: 3935–3948.

[5] Al-Saydeh, S. A.; El-Naas, M. H.; Zaidi, S. J. (2017) Copper removal from industrial wastewater: A comprehensive review. *Journal of Industrial and Engineering Chemistry,* 56: 35–44.

[6] Al-Rashdi, B.; Somerfield, C.; Hilal, N. (2011) Heavy metals removal using adsorption and nanofiltration techniques. *Separation & Purification Reviews,* 40 (3): 209-259.

[7] Qdaisa, H.A.; Moussa, H. (2004) Removal of heavy metals from wastewater by membrane processes: a comparative study. *Desalination,* 164: 105-110.

[8] Li, X.; Liu, Y.; Wang, J.; Gascon, J.; Li, J.; Van der Bruggen, B. (2017) Metal– organic frameworks based membranes for liquid separation. *Chemical Society Reviews,* 46: 7124–7144.

[9] Echaide-Górriz, C.; Sorribas, S.; Téllez, C.; Coronas, J. (2016) MOF nanoparticles of MIL-68 (Al), MIL-101 (Cr) and ZIF-11 for thin film nanocomposite organic solvent nanofiltration membranes. *RSC Advances,* 6 (93): 90417-90426.

[10] Wang, X.; Zhai, L.; Wang, Y.; Li, R.; Gu, X.; Yuan, Y.D.; Qian, Y.; Hu, Z.; Zhao, D. (2017) Improving Water-Treatment Performance of Zirconium Metal-Organic Framework Membranes by Post synthetic Defect Healing. *ACS applied materials & interfaces,* 9 (43): 37848-37855.

[11] Ma, J.; Guo, X.; Ying, Y.; Liu, D.; Zhong, C. (2017) Composite ultrafiltration membrane tailored by MOF@ GO with highly improved water purification performance. *Chemical Engineering Journal,* 313: 890-898.

[12] Rivera, J.M.; Rincón, S.; Ben Youssef, C.; Zepeda, A. (2016) Highly Efficient Adsorption of Aqueous Pb (II) with Mesoporous Metal-Organic Framework-5: An Equilibrium and Kinetic Study. *Journal of Nanomaterials,* 2016.

[13] Ming, Y.; Purewal, J.; Yang, J.; Xu, C.; Soltis, R.; Warner, J.; Veenstra, M.; Gaab, M.; Müller, U.; Siegel, D.J. (2015) Kinetic stability of MOF-5 in humid environments: impact of powder densification, humidity level, and exposure time. *Langmuir,* 31 (17): 4988-4995.

[14] Mahdi, E.M.; Tan, J.C. (2016) Dynamic molecular interactions between polyurethane and ZIF-8 in a polymer-MOF nanocomposite: Microstructural, thermo-mechanical and viscoelastic effects. *Polymer,* 97: 31-43.

392 [15] Mueller, U.; Schubert, M.; Teich, F.; Puetter, H.; Schierle-Arndt, K.; Pastre, J. (2006)
393 Metal–organic frameworks prospective industrial applications. *Journal of Materials*
394 *Chemistry,* 16: 626–636.
395 [16] Jonsson, G.; Boesen, C.E. (1977) Concentration polarization in a reverse osmosis test
396 cell. *Desalination,* 21 (1): 1-10.
397 [17] Iswarya, N.; Kumar, M.G.; Rajan, K.S.; Balaguru, R.J.B. (2012) Synthesis,
398 characterization and adsorption capability of MOF-5. *Asian Journal of Scientific*
399 *Research,* 5 (4): 247-254.
400 [18] Abdel-Karim, A.; Gad-Allah, T.A.; El-Kalliny, A.S.; Ahmed, S.I.; Souaya, E.R.;
401 Badawy, M.I.; Ulbricht, M. (2017) Fabrication of modified polyethersulfone
402 membranes for wastewater treatment by submerged membrane bioreactor. *Separation*
403 *and Purification Technology,* 175: 36-46.
404 [19] Rodrigues Filho, G.; Monteiro, D.S.; da Silva Meireles, C., de Assunção, R.M.N.;
405 Cerqueira, D.A.; Barud, H.S.; Ribeiro, S.J.; Messadeq, Y. (2008) Synthesis and
406 characterization of cellulose acetate produced from recycled newspaper. *Carbohydrate*
407 *Polymers,* 73 (1): 74-82.
408 [20] Zhao, C.; Xu, X.; Chen, J.; Yang, F. (2013) Effect of graphene oxide concentration on
409 the morphologies and antifouling properties of PVDF ultrafiltration membranes.
410 *Journal of Environmental Chemical Engineering,* 1 (3): 349-354.
411 [21] Tirmizi, S.A.; Badshah, A.; Ammad, H.M.; Jawad, M.; Abbas, S.M.; Rana, U.A.; Khan,
412 S.U.D. (2018) Synthesis of highly stable MOF-5@ MWCNTs nanocomposite with
413 improved hydrophobic properties. *Arabian Journal of Chemistry,* 11 (1): 26-33.
414 [22] Abedini, R.; Mousavi, S. M.; Aminzadeh, R. (2011) A novel cellulose acetate (CA)
415 membrane using TiO_2 nanoparticles: Preparation, characterization and permeation
416 study. *Desalination,* 277: 40–45.

[23] Boussu, K. ; Van der Bruggen, B.; Volodin, A.; Van Haesendonck, C.V.; Delcour, J.A.; Van der Meeren, P.; Vandecasteele, C. (2006) Characterization of commercial Nanofiltration membranes and comparison with self-made polyethersulfone membranes. *Desalination,* 191: 245–253.

[24] Nikooe, N.; Saljoughi, E. (2017) Preparation and characterization of novel PVDF Nanofiltration membranes with hydrophilic property for filtration of dye aqueous solution. *Applied Surface Science,* 413: 41–49.

[25] Shen, L.; Bian, X.; Lu, X.; Shi, L.; Liu, Z.; Chen, L.; Hou, Z.; Fan, K. (2012) Preparation and characterization of ZnO/polyethersulfone (PES) hybrid membranes. *Desalination,* 293: 21-29.

[26] Rahimpour, A.; Jahanshahi, M.; Khalili, S.; Mollahosseini, A.; Zirepour, A.; Rajaeian, B. (2012) Novel functionalized carbon nanotubes for improving the surface properties and performance of polyethersulfone (PES) membrane. *Desalination,* 286: 99–107.

[27] Wua, G.; Gan, S.; Cui, L.; Xu, Y. (2008) Preparation and characterization of PES/TiO2 composite membranes. *Applied Surface Science,* 254: 7080–7086.

[28] Sotto, A.; Orcajo, G.; Arsuaga, J.M.; Calleja, G.; Landaburu-Aguirre, J. (2015) Preparation and characterization of MOF-PES ultrafiltration membranes. *Journal of Applied Polymer Science,* 132 (21).

[29] Zeng, G.; Ye, Z.; Hea, Y.; Yang, Xi; Maa, J.; Shi, H.; Feng, Z. (2017) Application of dopamine-modified halloysite nanotubes/PVDF blend membranes for direct dyes removal from wastewater. *Chemical Engineering Journal,* 323: 572–583.

Table caption

TABLES

Membrane type	Composition of casting solutions		
	Polymer (g)	MOF-5 (g)	DMF solvent (ml)
Neat PES	4.375	-	21.7
PES+ 0.5% MOF-5	4.353	0.022	21.7
Neat PVDF	4.375	-	21.7
PVDF+0.5% MOF-5	4.353	0.022	21.7
Neat CA	4.375	-	21.7
CA+ 0.5% MOF-5	4.353	0.022	21.7

Table 1. Composition of casting solution for the preparation of composite membranes

Feed solution	K	D
Copper solution	5.78×10^{-5} m/s	4.335×10^{-9} m^2/s
Cobalt solution	4.22×10^{-5} m/s	4.182×10^{-9} m^2/s

Table 2. Mass transfer coefficient (K) and diffusion coefficient (D)

Membranes	Porosity (%)	Mean Pore radius (nm)
PES	70.50	5.62
PES/MOF-5	78.94	6.97
CA	72.50	5.57
CA/MOF-5	81.26	9.09
PVDF	65.32	3.92
PVDF/MOF-5	74.40	4.30

Table 3. Porosity and mean pore radius of membranes

Membranes	Contact Angle (°)
PES/MOF-5	76.42
CA/MOF-5	70.68
PVDF/MOF-5	72.975
PES	86.075
CA	75.03
PVDF	80.47

Table 4. Contact angle measurement

Membrane Type	Membranes Resistance, R_m (m^{-1})	Pure water flux (L/m^2 hr)
PES	13×10^{13}	29.52±1.6
PES/MOF-5	7.4×10^{13}	53.31±1.6
CA	9.6×10^{13}	41.01±1.2
CA/MOF-5	5.6×10^{13}	69.72±1.4
PVDF	17×10^{13}	22.96±1.4
PVDF/MOF-5	11×10^{13}	33.63±1.2

Table 5. Membrane resistance and pure water flux

Membrane Type	C_m (ppm)	Rejection percentage (%)	
		R_{obs}	R_{real}
PES	1178.14	30.5	35.35
PES/MOF-5	1075.12	51.4	58.74
CA	1111.97	50.8	52.39
CA/MOF-5	1033.57	53.3	58.00
PVDF	1072.63	52.3	55.52
PVDF/MOF-5	1039.91	54.3	56.05

Table 6. Cu (II) rejection of membranes

Membranes type	C_m (ppm)	Rejection Efficiency %	
		R_{obs} (%)	R_{real} (%)
PES	1084.29	58.35	61.58
PES/MOF-5	1225.31	74.40	79.10
CA	1079.60	45.30	49.34
CA/MOF-5	1353.49	77.0	83.00
PVDF	1040.16	41.8	44.04
PVDF/MOF-5	1116.93	64.20	67.94

Table 7. Co (II) rejection of membranes

Figure caption

Scheme. 1. Schematic representation of removal of heavy metal ions from aqueous solution by MOF-5 incorporated membranes Nanofiltration.

Scheme

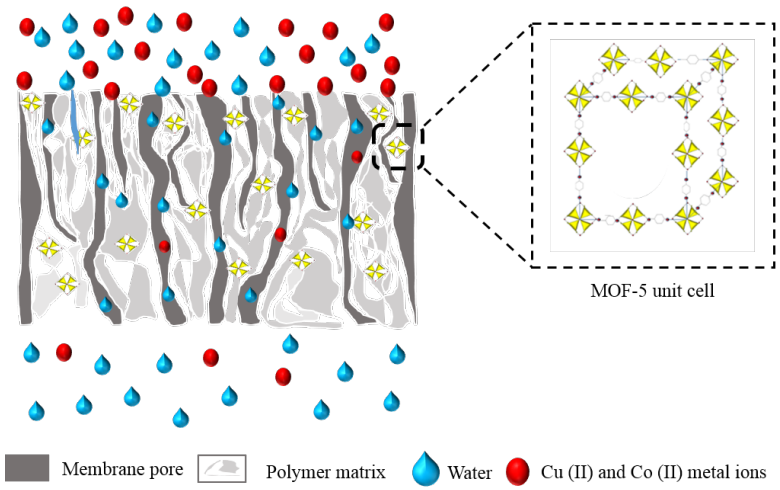

Scheme. 1. Schematic representation of removal of heavy metal ions from aqueous solution by MOF-5 incorporated membranes Nanofiltration.

FIGURES

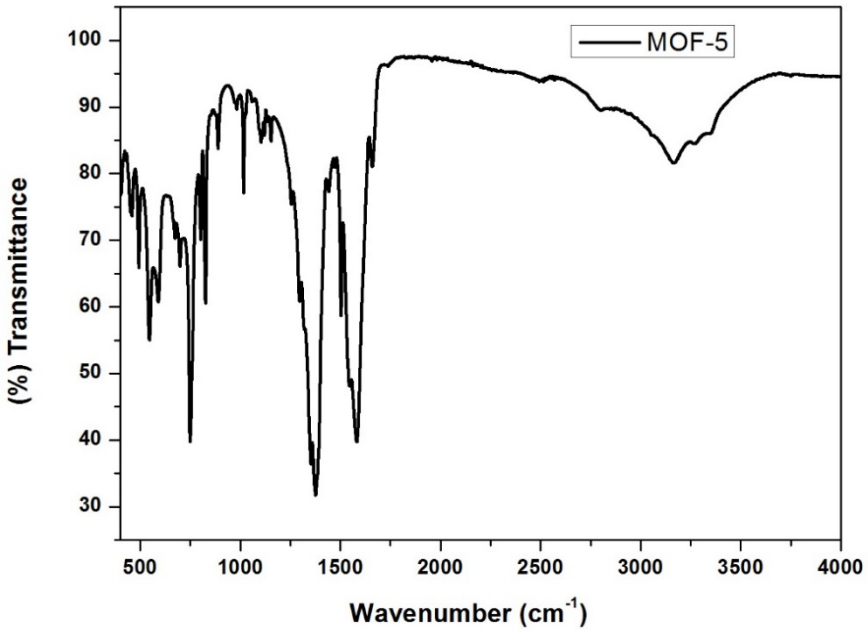

Figure 1. FTIR spectra of MOF-5

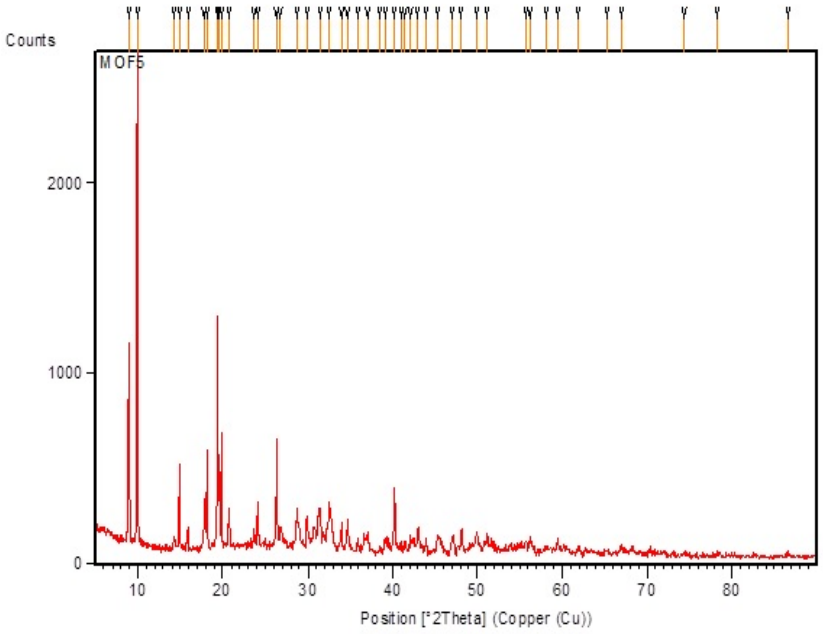

Figure 2. XRD image of MOF-5

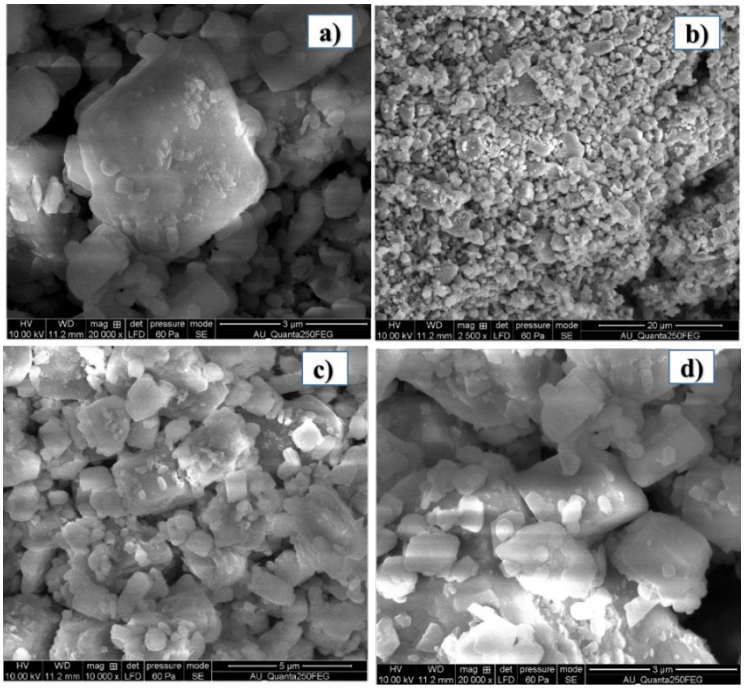

Figure 3. SEM image of MOF-5

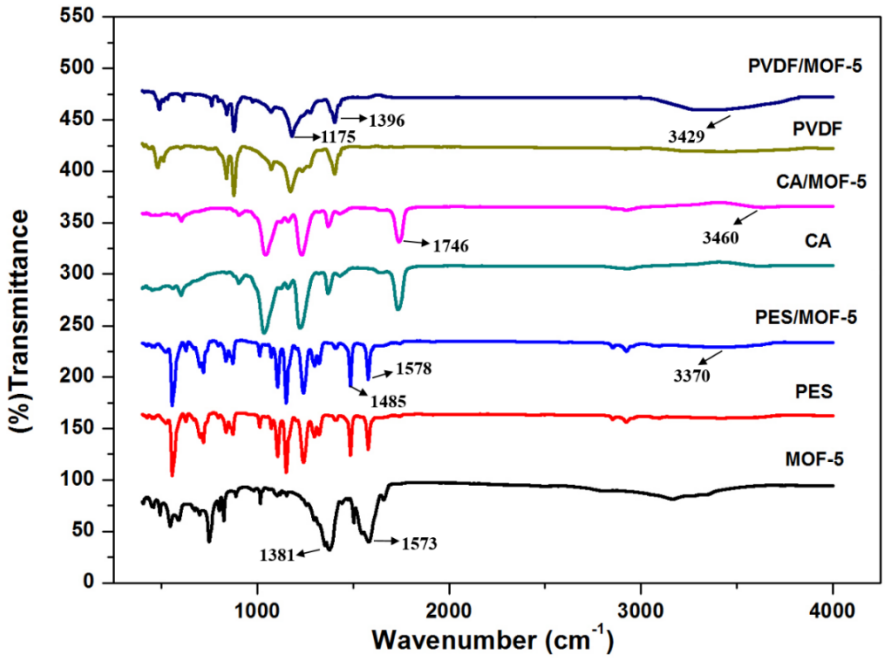

Figure 4. FT-IR spectra of MOF-5 and membranes

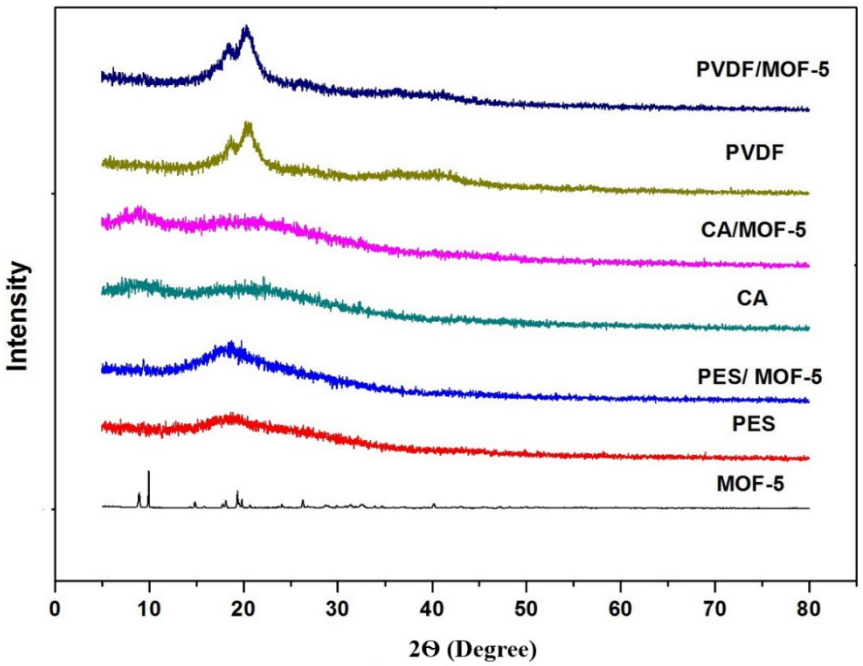

587

588 Figure 5. XRD analysis of MOF-5 and membranes

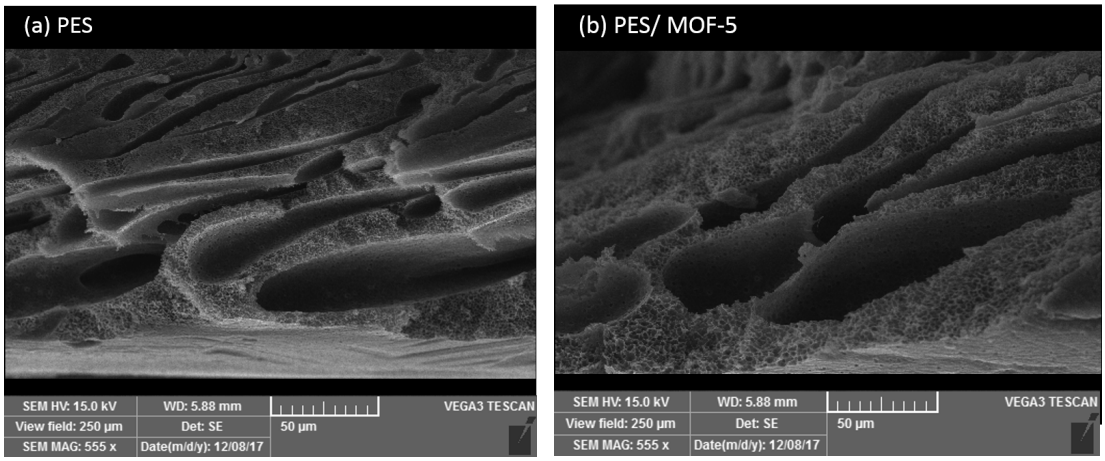

593

594 Figure 6. Cross-sectional view of (a) neat PES and (b) PES/MOF-5

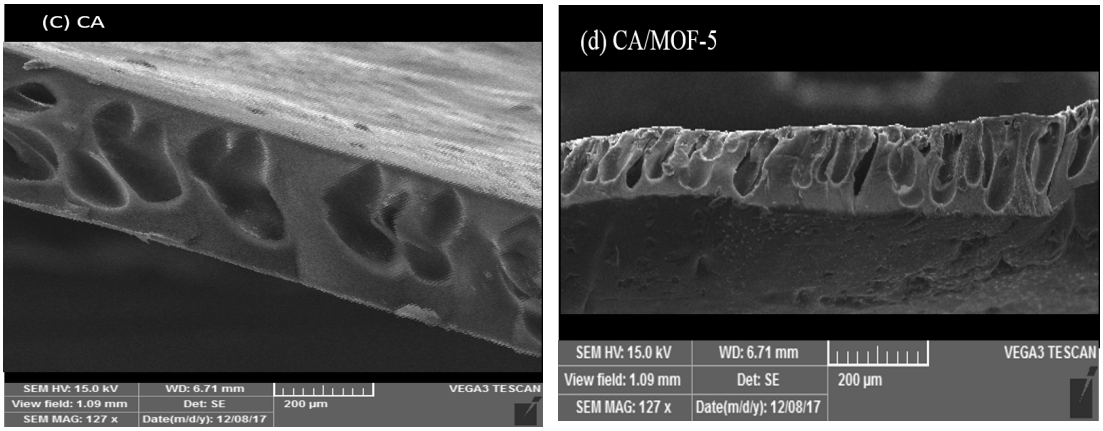

600 Figure 7. Cross-sectional view of (c) neat CA and (d) CA/MOF-5

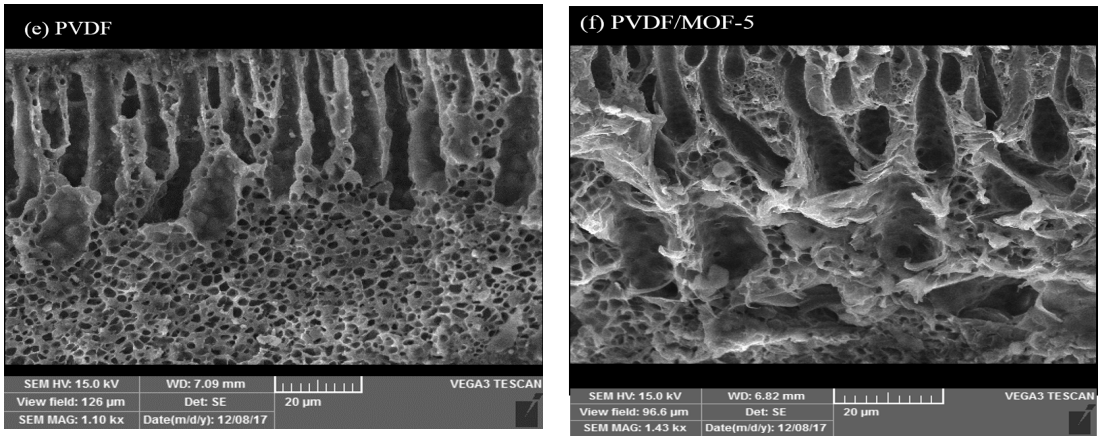

605 Figure 8. Cross-sectional Image of (e) neat PVDF and (f) PVDF/MOF-5

606

607

608

609

610

611

612

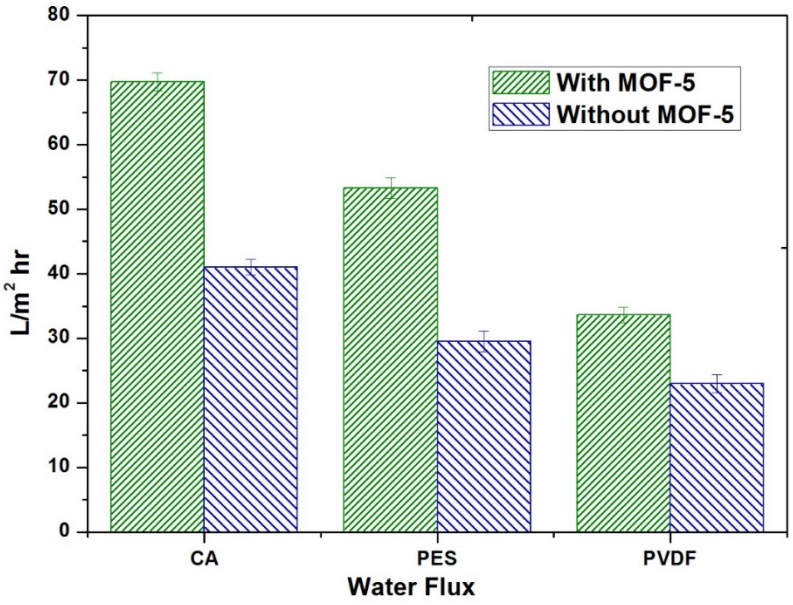

613 Figure 9. Pure water flux of membranes

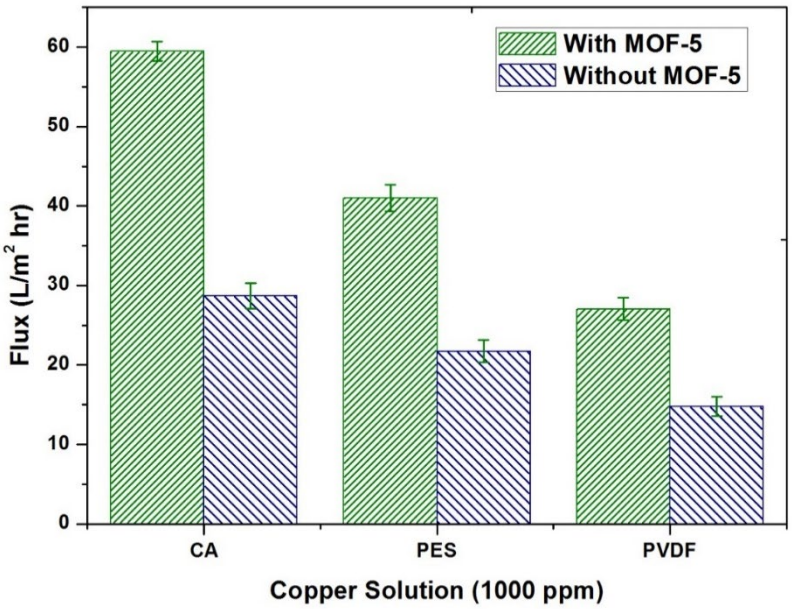

Figure 10. Flux of copper feed solution for membranes

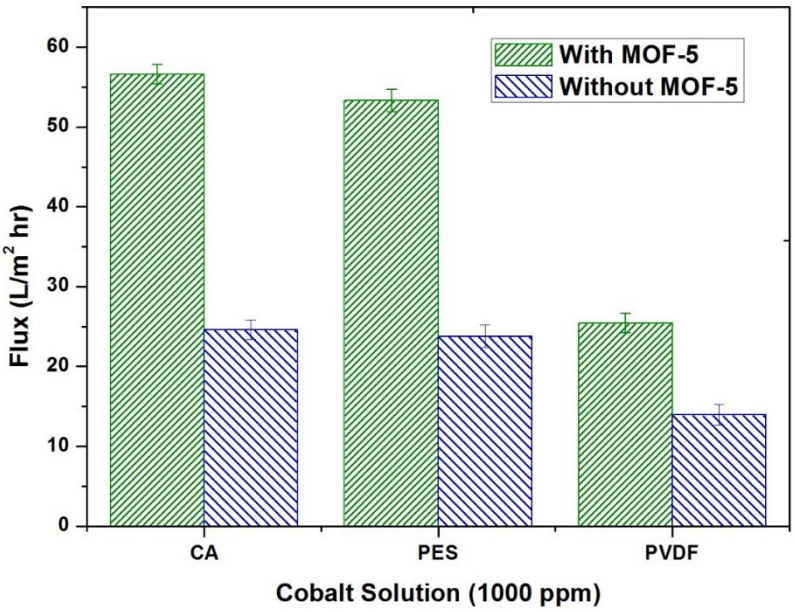

Figure 11. Flux of cobalt feed solution for membranes